



ORIGINAL ARTICLE

# Histological, immunohistochemical and radiographic evaluation of Amitriptyline administration on the periodontium of albino rats (An experimental study)



Rabab Hassan<sup>a,\*</sup>, Naglaa Fathallah Ahmed<sup>b</sup>, Safaa Ismail Hussein<sup>c</sup>

<sup>a</sup> Associate professor of Oral Biology, Faculty of Dentistry, Ain Shams University, Cairo, Egypt

<sup>b</sup> Lecturer of Oral Radiology, Faculty of Dentistry, Ain Shams University, Cairo, Egypt

<sup>c</sup> Lecturer of Oral Biology, Faculty of Dentistry, Ain Shams University, Cairo, Egypt

Received 6 June 2022; revised 26 June 2022; accepted 28 June 2022

Available online 4 July 2022

## KEYWORDS

Amitriptyline;  
Osteopontin;  
Periodontium;  
Cone beam CT;  
HU value

**Abstract** *Background:* Amitriptyline is a tricyclic antidepressant drug accustomed to treat depressive disorders. It recorded many side effects on different tissues.

*Objective:* To investigate reaction of Albino rats' periodontium after oral administration of Amitriptyline histologically and radiographically.

*Methods:* Fourteen adult male albino rats (150–200 g) were divided into two groups, control and experimental. Rats of experimental group received 10 mg/kg/day of Amitriptyline hydrochloride by oral gavage for four weeks. Mandibles were prepared for hematoxylin and eosin (H&E) and anti-osteopontin (Anti-OPN) immunohistochemistry staining. Bone mineral density was measured in mandibular alveolar bone. Statistical analysis for Anti-OPN and relative Hounsfield unit value (HU value) was performed using independent-samples *t*-test.

*Results:* Gingiva of experimental group showed epithelial degeneration with pyknotic nuclei and disintegration in lamina propria. Areas of separation in alveolar bone and degeneration of some regions in cementum were seen with apparent increase in periodontal ligament (PDL) thickness and its detachment from bone and cementum at some regions. Immunohistochemical examination of experimental group showed apparently increased immunopositivity in gingiva, cementocytes,

\* Corresponding author.

E-mail address: [rabab.hassan@dent.asu.edu.eg](mailto:rabab.hassan@dent.asu.edu.eg) (R. Hassan).

Peer review under responsibility of King Saud University.



Production and hosting by Elsevier

osteocytes, cementum, bone matrices, fibroblasts and PDL fibers when compared to control group. Statistical analysis revealed insignificant difference of Anti-OPN area% in gingiva between both studied groups. While there was statistical significant increase of Anti-OPN area% in the other periodontium tissues and high statistical significant decrease of relative HU value in experimental group when compared to control.

**Conclusions:** Amitriptyline has destructive effect on periodontal tissues and statistically increases the expression of Anti-OPN in all periodontal tissues except gingiva and decreases bone mineral density.

© 2022 The Authors. Production and hosting by Elsevier B.V. on behalf of King Saud University. This is an open access article under the CC BY-NC-ND license (<http://creativecommons.org/licenses/by-nc-nd/4.0/>).

## 1. Introduction

Periodontium consists of four main components: gingiva, alveolar bone, periodontal ligament (PDL) and cementum (Madukwe, 2011). Osteopontin (OPN) is a member of the Small Integrin-Binding Ligand N-linked Glycoprotein of mineralized tissue-associated proteins and is expressed in periodontium (Fisher & Fedarko, 2003; Gaballah et al., 2018). It regulates mineralization in vitro and in vivo (Boskey et al., 2002; Holm et al., 2014).

During various pathological conditions affecting periodontium “such as gingivitis, chronic periodontitis, aggressive periodontitis and necrotizing ulcerative gingivitis and periodontitis” (Kinane et al., 2017), OPN showed increased expression helping in maintaining tissue integrity as it is required for stress-induced bone remodeling and adhesion of osteoclasts during resorption (Teitelbaum, 2000; Denhardt et al., 2001).

Depressive disorders can worsen patient’s condition with chronic illness (Evans et al., 2005). Depression produces a great decline in health if compared to chronic diseases such as angina, asthma, arthritis and diabetes (Moussavi et al., 2007). Antidepressants are classified as: first-generation: including monoamine oxidase inhibitors and tricyclic or tetracyclic antidepressants and second-generation: including selective serotonin reuptake inhibitors (SSRIs), selective norepinephrine reuptake inhibitors and atypical antidepressants (Yekehtaz et al., 2013).

As one of tricyclic antidepressants (TCAs), Amitriptyline inhibits the presynaptic reuptake of serotonin and norepinephrine resulting in increasing these neurotransmitters concentrations at synaptic cleft (Su et al., 2015). Amitriptyline can activate the signaling of fibroblast growth factor receptor in glial cells which shares in its antidepressant action (Hisaoka et al., 2011).

Beside the antidepressant action of Amitriptyline, it shows other pharmacological effects such as anti-inflammatory (Hajhashemia et al., 2008) and analgesic effects (Paudel et al., 2007), which relieves pain of exposed dentin (Aminsobhani et al., 2016) and oral mucositis (kakoei et al., 2018). Yet, it has different side effects such as reduction in bone mineral density (BMD) and (or) an increased risk of bone fractures (Ortuño et al., 2016). Beside constipation, dizziness, dry mouth, blurred vision, urinary retention, weight gain, orthostatic hypotension and cardiotoxicity (Chaudhry et al., 2017; Buhagiar et al., 2019).

From above mentioned data, this study aimed to appraise the effect of Amitriptyline on albino rat periodontium tissues

through histological, immunohistochemical and radiographic analysis.

## 2. Materials and methods:

The experiment was performed according to guidelines of Ethics Committee, Faculty of Dentistry, Ain Shams University. The ethical approval number is (FDASU-Rec IR042207).

### 2.1. Materials

#### 2.1.1. Animals

Fourteen adult Wistar male albino rats weighing between 150 and 200 g (8–12 weeks) were used and housed in separate cages, five rats per cage in Animal House of Medical Research Center - Ain-Shams University under supervision of specialized veterinarian. Rats were kept under good ventilation and adequate stable diet of fresh vegetables, dried bread and tap water ad libitum throughout the experimental period.

#### 2.1.2. Amitriptyline hydrochloride (10 mg tablet)

Amitriptyline hydrochloride (10 mg tablet) Was purchased in form of Tryptizol tablets from (Kahira Pharm. & Chem. Ind. Co., Cairo, Egypt).

### 2.2. Methods

After a week of acclimatization, rats were randomly divided into two groups (seven rats each) as follows:

- **Control group (C G):**

Rats received distilled water by oral gavage.

- **Experimental group (Ex G):**

Rats received Amitriptyline hydrochloride by oral gavage with dose (10 mg/kg/day) dissolved in 4 ml distilled water for four weeks (Elsharkawy & Alhazzazi, 2016; Abd AIObaidi et al., 2021).

#### 2.2.1. Samples preparation

At the end of experimental period, rats were sacrificed by overdose of anesthesia (ketamine), and mandible was dissected and divided into two halves. The right half (molar area) was fixed in 10% phosphate buffered formalin solution for 5 days,

washed then placed in ethylene diamine tetra-acetic acid for decalcification and stained with hematoxylin and eosin (H&E) and Anti-OPN immunohistochemical marker. While the left half was imaged by cone beam computed tomography (CBCT).

**2.2.1.1. H&E stain.** After decalcification, specimens were washed under running water, dehydrated by ascending concentrations of alcohol then transferred to xylol. Specimens were infiltrated and embedded in the center of paraffin wax blocks then sectioned by microtome (4  $\mu\text{m}$  thick). Sections were rehydrated and stained by H&E stain (Bancroft et al., 2013).

**2.2.1.2. Anti-OPN immunohistochemical stain.** Sections were mounted on positive charged slides, then rehydrated, rinsed and bathed with 0.3%  $\text{H}_2\text{O}_2$  for 15 min to inactivate endogenous peroxidase. Afterwards, sections were incubated with 1:10 normal swine serum for 30 min to block non-specific staining. Rabbit polyclonal Anti-OPN was diluted in phosphate buffered saline (PBS), containing 0.1% bovine serum albumin (1:2000) and incubated at 4°C for 18 h. Then, sections were rinsed twice for 3 min with PBS solutions that contained 0.01% Triton X-100 and once for 3 min with plain PBS. Sections were incubated with a biotinylated goat anti-body (DAKO LSAB Kit, USA) for 15 min, rinsed with PBS, and incubated with streptavidin peroxidase conjugate for 15 min. Anti-body complexes were visualized after adding buffered diaminobenzidine (Sigma-Aldrich®, USA) substrate for 3 min. Sections were counterstained with Mayer's hematoxylin, dehydrated with ascending alcohols, cleared with xylene and mounted with cover slips using DPX. Positive reaction appeared as brown cytoplasmic staining (Ivanovski et al., 2001).

Sections were examined and photographed at 200 $\times$  and 400 $\times$  magnifications using light microscope (Olympus® BX 60, Tokyo, Japan).

### 2.2.2. Histomorphometric analysis

Image analysis software (Image J, 1.41a, NIH, USA) was used to calculate Anti-OPN area%. Three different representative fields from each slide per rat of studied groups were selected. Area of each examined field was 0.77  $\text{mm}^2$  at magnification x200 for gingiva and 0.19  $\text{mm}^2$  at magnification x400 for alveolar bone, PDL and cementum. After grey calibration, the image was transformed into a grey delineated image, positive reactivity was chosen then masked by a blue binary color.

### 2.2.3. Radiographic analysis of BMD

Left halves of mandibles were imaged using CBCT at Oral Radiology Department, Faculty of Dentistry, Ain Shams University. Scans were obtained by (Planmeca ProMax® 3D s) system at (90Kvp, 12 mA, 15sec, 150  $\mu\text{m}$  voxel size) and image size 5  $\times$  8 cm. Reconstructed data sets were exported as Digital Imaging and Communications in Medicine (DICOM) image stacks and then transferred to another workstation to view images using On Demand software (On demand 3D™, Cybermed, South Korea). First, Image brightness and contrast were adjusted. Bone density/gray scale value was measured in two points as relative Hounsfield unit value (HU value), mesial and distal to the second molar, just below

cement-enamel junction. Then, the mean of two measurements was calculated (Fig. 1a).

### 2.2.4. Statistical analysis

Data from histomorphometric and radiographic analysis were analyzed using statistical package for social sciences, version 23.0 (SPSS Inc., Chicago, Illinois, USA). Quantitative data were presented as mean  $\pm$  standard deviation and ranges. Data were explored for normality using Kolmogorov-Smirnov and Shapiro-Wilk Test. Independent-samples *t*-test of significance was used for comparing between two means & Mann Whitney *U* test: for two-group comparisons in non-parametric data. Confidence interval was set to 95% and the margin of error accepted was set to 5%. *p*-value was considered significant at <0.05, highly significant at <0.001 and insignificant at >0.05.

## 3. Results

### 3.1. H&E results

Histological examination of control group revealed gingival mucosa covered with keratinized stratified squamous epithelium that showed short columnar basal cell layer resting on well-defined basement membrane, polygonal prickle cells and flattened granular cell layer covered by thin and regular esinophilic keratin layer. Some clear cells were detected within epithelium. Lamina propria appeared dense and fibrous. Long and slender connective tissue (c.t) papillae and spindle shaped fibroblasts were observed (Fig. 1b). Alveolar process showed regular margin, Haversian canal and fibrocellular marrow cavities. Homogenous acellular cementum with even thickness and well organized PDL were observed (Fig. 1c). Alveolar bone proper was lined with plump osteoblasts. Numerous osteocytes lacunae were noticed. PDL appeared dense with oblique direction. Spindle shaped fibroblasts were overlying PDL fibers. Cuboidal shaped cementoblasts lined acellular cementum surface and incremental lines of Salter were noticed (Fig. 1d). Cellular cementum showed cementocytes lacunae; some were plump while others were flattened (Fig. 1e).

Examination of experimental group showed gingival epithelium with detectable reduction in thickness in some parts. Apparent shrinkage in rete pegs was detected and basement membrane was ill-defined. Basal cell layer appeared flattened; some showed loss of polarity while others showed pyknotic nuclei. Some cells with clear cytoplasm, pyknotic nuclei and few mitotic figures were seen within prickle cell layer. Areas of disintegration were seen within the lamina propria and c.t papillae which were numerous, slender and long reaching deeply in the epithelium. Fibroblasts showed apparent reduction in their size and number (Fig. 2a). Some specimens showed apparently increased epithelial thickness with cell nests and detached keratin (Fig. 2b). Alveolar margin appeared irregular. Areas of separation in bone and reversal lines were observed. Acellular cementum showed uneven thickness. Apparent increase in PDL thickness with detachment of PDL from bone and cementum at some regions was detected (Fig. 2c). Degeneration of some regions in acellular cementum and absence of cementoblastic lining were seen. PDL appeared disorganized and almost parallel to cementum surface with few widened blood vessels (Fig. 2d).

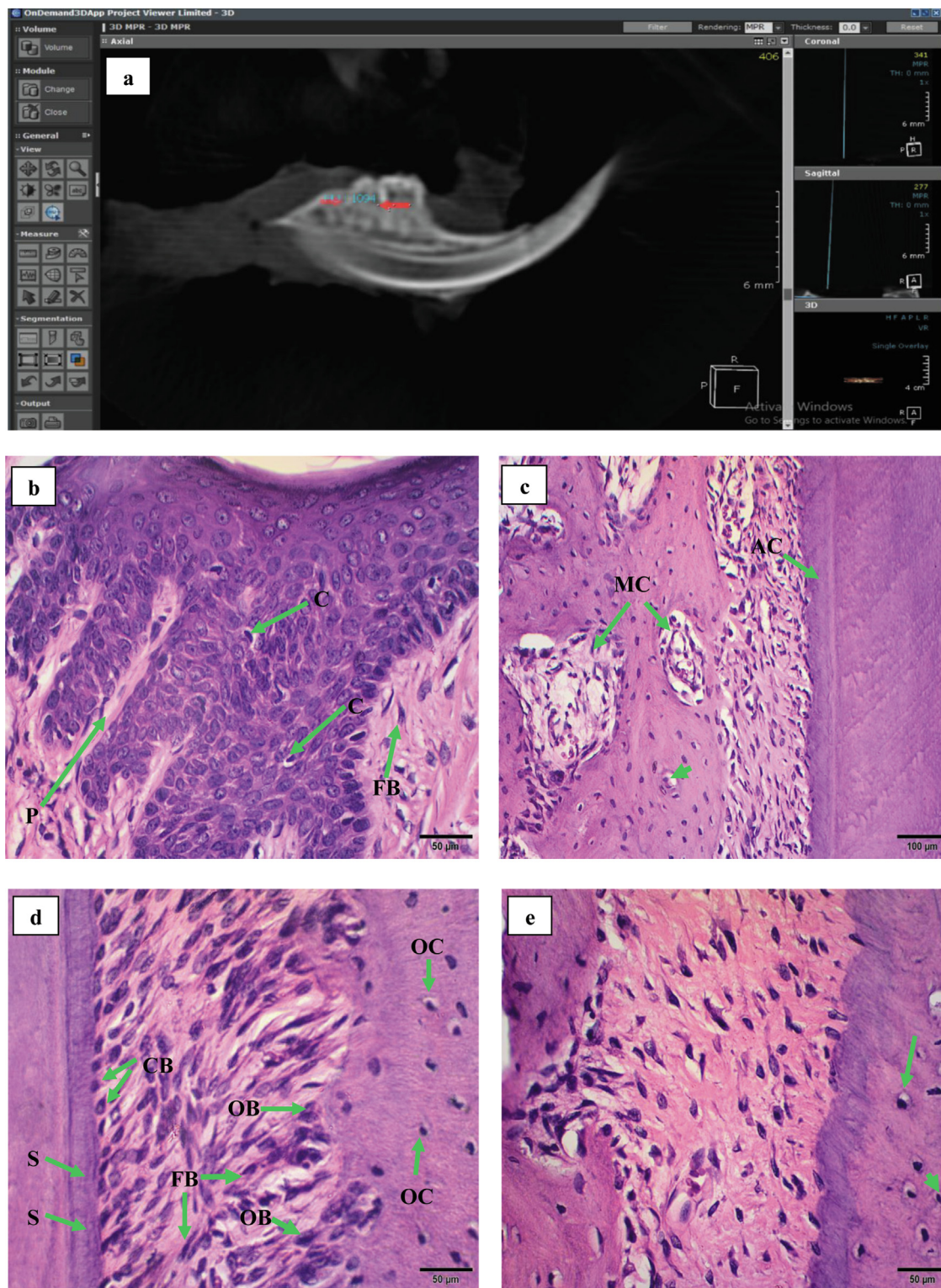


**Fig. 1** (a)- CBCT of the mandibular specimen showing standardized areas to be evaluated (red arrows), mesial and distal to the second molar just below the CEJ. The HU value is measured in these two points then averaged. Photomicrographs of the control group showing (b)- Gingiva with keratinized stratified squamous epithelial covering. Thin and regular eosinophilic keratin layer, clear cells (C). Dense and fibrous lamina propria with long and slender c.t papillae (P) and spindle shaped fibroblasts (FB). (c)- Alveolar process with regular margin, Haversian canal (arrow head) and fibrocellular marrow cavities (MC). Homogenous acellular cementum with even thickness (AC) and well organized PDL. (d)-Alveolar bone proper with plump osteoblasts lining (OB), numerous osteocytes lacunae (OC). Spindle shaped fibroblasts (FB) overlying PDL fibers. Cuboidal shaped cementoblasts lining the surface of acellular cementum (CB), incremental lines of Salter (S). (e)-Cellular cementum with cementocytes lacunae, some are plump (arrow) while others are flattened (arrow head), (H&E, original magnification, (b, d & e)  $\times 400$ , (c)  $\times 200$ ).

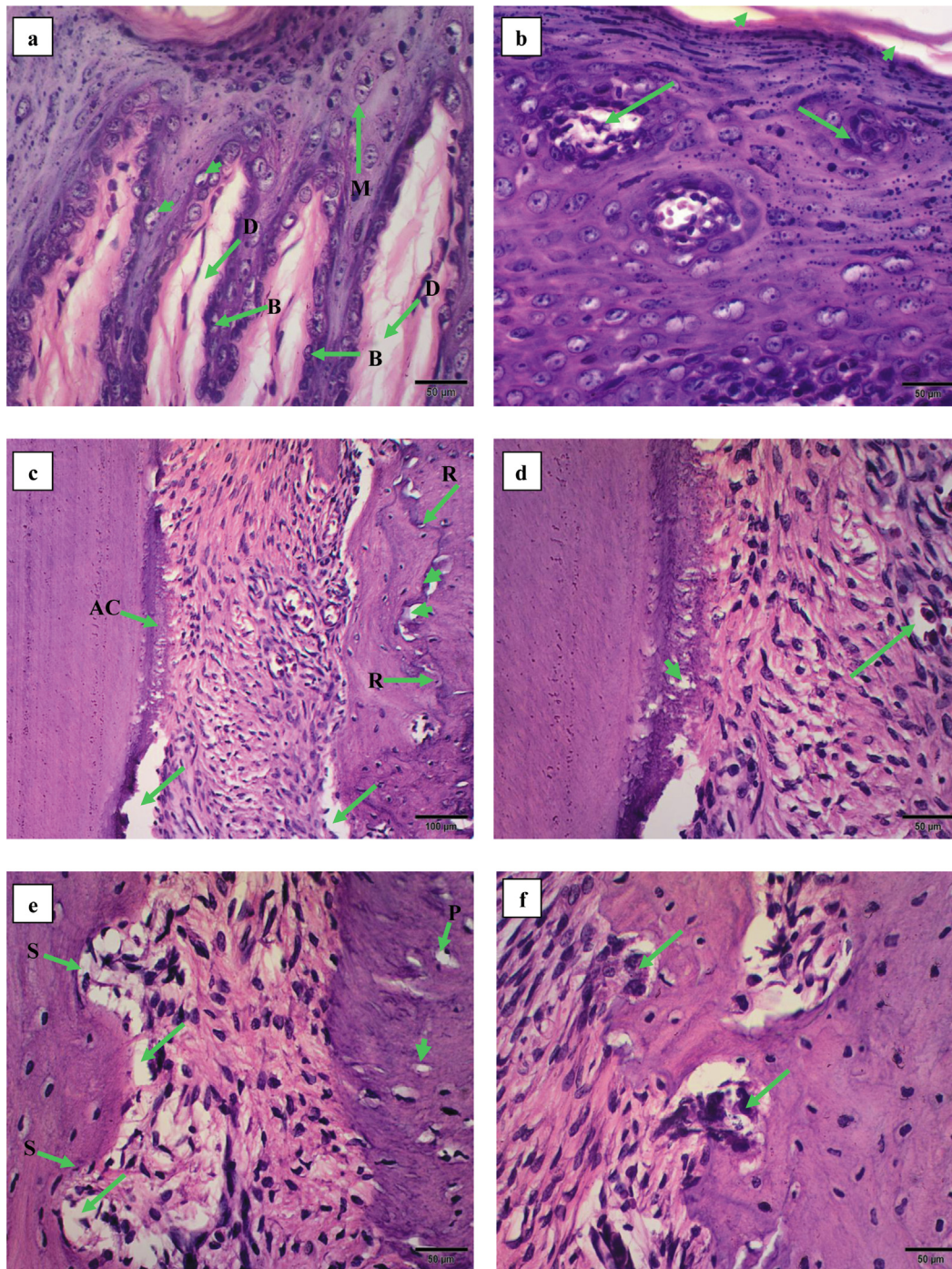


**Fig. 2** Photomicrographs of experimental group showing: (a)-Gingiva with basal cells with pyknotic nuclei (B) resting on ill-defined basement membrane. Cells with clear cytoplasm and pyknotic nuclei (arrow heads) and few mitotic figures (M). Areas of disintegration in c.t. papillae (D). (b)-Cell nests (arrows) and detached keratin layer (arrow heads). (c)-Alveolar process with irregular margin, areas of separation in bone (arrow heads) and reversal lines (R). Acellular cementum with uneven thickness (AC). Detectable increase in PDL thickness with detachment of PDL from bone and cementum at some regions (arrows). (d)-Degeneration of some regions in acellular cementum (arrow head) and absence of cementoblastic lining. Disorganized PDL with few widened blood vessels (arrow). (e)-Areas of degeneration in PDL (arrows). Cellular cementum with cementocytes lacunae some empty (arrow head), while others showing pyknotic nuclei (P). Scalloped alveolar bone margin (S). (f)- Osteoclasts in Howship's lacunae (arrows). (H&E, original magnification, (a, b, d, e & f) x400, (c) x200).

PDL in the region of cellular cementum showed areas of degeneration with loss of regular orientation of its fiber bundles. Some cementocytes lacunae appeared empty while

others showed pyknotic nuclei. Alveolar bone margin appeared scalloped (Fig. 2e). Alveolar bone showed many osteoclasts in Howship's lacunae (Fig. 2f).

### 3.2. Immunohistochemical results

Histological examination of Anti-OPN of gingiva in control group showed cytoplasmic immunopositive reactivity in all epithelial layers especially in basal and prickle cell layers. Positive reaction was also detected in some c.t. cells (Fig. 3a). Regarding alveolar bone, cementum and PDL, very few positive immuno-reactivity was detected in cementocytes, fibroblast and bone matrix. PDL fibers showed some positive immuno-staining (Fig. 3b).

Gingiva of experimental group showed apparently increased immunopositivity in epithelium and in c.t. cells (Fig. 3c). Increased positive immuno-staining was noticed in cementocytes, osteocytes, cementum and bone matrices, fibroblasts and PDL fibers (Fig. 3d).

### 3.3. Statistical results

Statistical analysis of Anti-OPN immunoreactivity area% revealed statistical insignificant difference in gingiva between two groups. While there was statistical significant increase of

Anti-OPN area% in bone, PDL and cementum of experimental group in comparison to control group (Table 1 & Fig. 4a). Furthermore, there was high statistical significant decrease of HU value in experimental group compared to control group (Table 2 & Fig. 4b).

## 4. Discussion

Depression is a mental problem that needs antidepressant drugs to balance neurotransmitters in brain (Rashid & Heider, 2008; El Atrash et al., 2019). Amitriptyline was the drug of choice in this study because it is widely used TCA and has same efficacy as second generation through inhibiting neurotransmitters "serotonin-norepinephrine" reuptake (Barbui & Hotopf, 2001; Tousson et al., 2018).

The CBCT allows rapid scan time, dose reduction, provides isotropic voxels and produces precise sub-millimeter resolution (Venkatesh & Elluru, 2017). BMD could be estimated by CBCT as mineral contents within apparent volume of bone to evaluate bone quantity and to estimate bone diseases (Kim, 2014; El Saadawy et al., 2019).

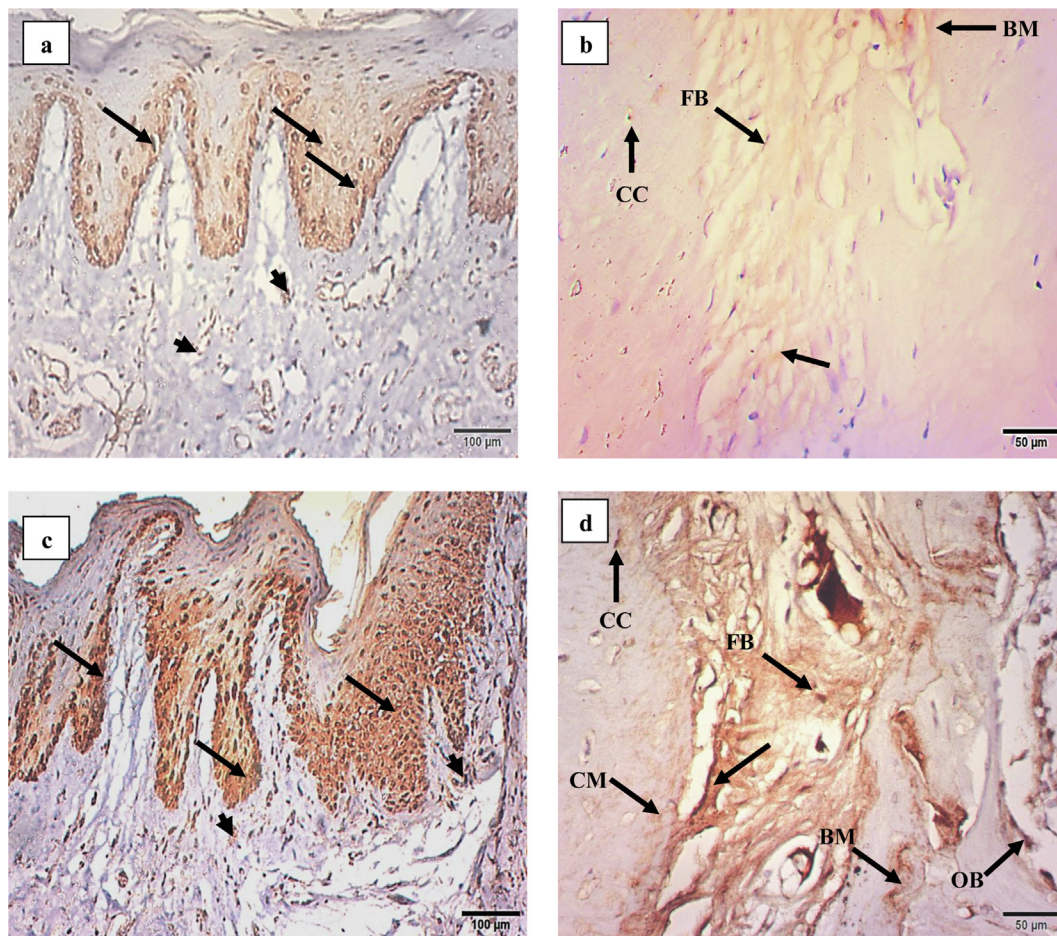


**Fig. 3** Photomicrographs showing: (a)- Gingiva of control group with positive immuno-reactivity in epithelium especially in basal and prickle cell layers (arrows). Note the presence of positive reaction in c.t. cells (arrow heads). (b)- Control group with very few positive immuno-reactions in cementocytes (CC), fibroblasts (FB), bone matrix (BM) and some staining in PDL fibers (arrow). (c)- Gingiva of experimental group with apparently increased immunopositivity in epithelium (arrows) and c.t. cells (arrow heads). (d)- Experimental group with positive immuno-staining in cementocytes (CC), osteoblasts (OB), cementum (CM) and bone (BM) matrices, fibroblasts (FB) and PDL fibers (arrow). (Anti-OPN, original magnification, (a & c) x200, (b & d) x400).

**Table 1** showing comparison between control and experimental groups according to area % of Anti-OPN immunoreactivity.

Area % of Anti-OPN immunoreactivity	Control Group (n = 7)	Experimental Group (n = 7)	U test	p-value
<b>Gingiva</b>				
Mean ± SD	9.48 ± 4.21	14.62 ± 7.34	-1.214	0.225
Range	1.59-13.07	7.09-27.98		
<b>Bone</b>				
Mean ± SD	1.16 ± 1.16	4.22 ± 3.07	-2.747	0.006*
Range	0.09-3.54	1.38-10.45		
<b>PDL</b>				
Mean ± SD	4.10 ± 2.95	19.57 ± 5.06	-3.130	0.002*
Range	0.03-7.15	12.87-28.36		
<b>Cementum</b>				
Mean ± SD	0.52 ± 0.54	2.06 ± 1.27	-2.492	0.013*
Range	0.01-1.54	0.78-4.43		

Using: U = Mann-Whitney test.  
 p-value > 0.05 NS.  
 \* p-value < 0.05 significant.

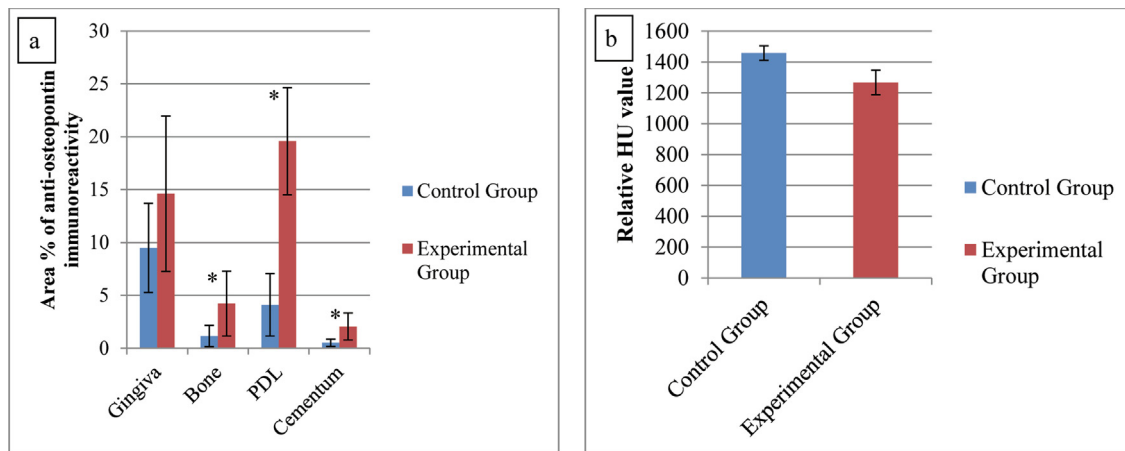


**Fig. 4** Bar charts showing comparison of mean and SD values between control and experimental groups (a)- Anti-OPN immunoreactivity area %. (b)- Relative HU value.

**Table 2** Showing comparison between control and experimental groups according to relative HU value.

Relative HU value	Control Group (n = 7)	Experimental Group (n = 7)	t-test	p-value
Mean ± SD	1457.71 ± 46.23	1267.14 ± 79.69	5.473	< 0.001**
Range	1404-1527	1145-1350		

Using: t-Independent Sample.  
 \*\* p-value < 0.001 highly significant.

Histological observation of gingiva in experimental group showed reduction in epithelium thickness in some parts while others showed increased epithelial thickness with cell nests. Ill-defined basement membrane, flattened basal cells, few mitotic figures within prickle cell layer and pyknotic nuclei and detached keratin were detected. Disintegration in lamina propria and c.t papillae and apparent reduction in fibroblasts size and number were seen. These epithelium and c.t changes coincide with Elsharkawy & Alhazzazi, (2016) who studied the effect of Amitriptyline with a dose

5 mg/kg and 10 mg/kg for eight weeks on submandibular salivary glands and reported atrophy and shrinkage of secretory portions and pyknotic basal flattened nuclei in ducts with severe widening of c.t septa.

Changes observed in epithelium and c.t in the current study could be related to the previously reported cytotoxic effects of Amitriptyline that cause degenerative changes and increase apoptotic cell death on salivary glands (Mubarak, 2012; Elsharkawy & Alhazzazi, 2016), and induce oxidative stress, mitochondrial dysfunction and increase the level of reactive

oxygen species and lipid peroxidation on cultured human primary fibroblasts (Cordero et al., 2009).

Histologically, alveolar margin of experimental group in this study was scalloped. Areas of separation in bone, reversal lines and osteoclasts were noticed. These findings coincide with Hanery & Blizotes, (2007) who reported detrimental effects of SSRIs drugs on bone density, size and formation. Our findings could be related to the inhibition of functional serotonin transporters in osteoblasts, osteoclasts, and osteocytes affecting bone metabolism and causing bone resorption and osteoporosis (Calarge et al., 2010; Warden et al., 2010).

Histological examination of PDL in our study revealed apparently its increased thickness with areas of disorganization and degeneration. These results are in parallel with de Almeida Prado et al., (2012) who found that 20 mg/kg of Amitriptyline increased fibrosis in bladder of infravesical obstruction model in rats. They related this fibrosis to increased collagen deposition.

In the present study, acellular cementum showed degeneration and appeared with uneven thickness. Absence of cementoblastic lining with some empty cementocytes lacunae and others with pyknotic nuclei was seen. These findings agree with Regueira et al., (2017) who correlated between SSRIs and periodontal cells. They suggested that periodontal cells are sensitive to Fluoxetine “a SSRIs” when taken with a dose 20 mg/kg during pregnancy and lactation and they reported reduction in cementoblasts, fibroblasts and osteoblasts quantities.

Immunohistochemical results in this study revealed increase of Anti-OPN area% in all studied tissues of experimental group in comparison to control group and this was statistically significant except for gingiva. These are in accordance with Kim et al., (2012) who reported increase of OPN expression during orthodontic tooth movement and linked that to increased bone resorption and tissue remodeling. So, our results could be related to destructive effect of Amitriptyline on periodontal tissues that caused bone resorption and degeneration of both PDL and cementum.

In the present study, HU value of the experimental group was significantly lower than that of control group. This was in accordance with Haney et al., (2007) and Diem et al., (2011) who investigated the effect of SSRIs on older men and women respectively. They found that BMD was lower among those reporting current SSRIs use in comparison to other antidepressants in men and increased fracture risk in women. Agacayak et al., (2019) reported a significant increase in dental volumetric tomography (DVT) cortical index and a significant decrease in HU cortical, HU spongiosis and DVT mandibular index values suggesting osteoporosis in patients treated with SSRIs for long time.

On the other hand, Saraykar et al., (2018) through their study on elderly women, did not observe any significant differences in BMD of elderly women but observed a tendency for a reduction in BMD at the spine level in SSRIs users.

To sum up, all findings recorded in the present study in periodontium of experimental group could be linked to the cytotoxic effects of Amitriptyline on periodontal cells, subsequently affecting regular functions of these cells causing all aforementioned histological, immunohistochemical and radiographic changes.

Further studies are needed by using preemptive drugs or herbs to ameliorate side effects of Amitriptyline on periodontium.

## 5. Conclusions

Amitriptyline has destructive effect on all periodontal tissues and results in disintegration of gingival lamina propria, alveolar bone resorption, disorganization of PDL and degeneration in cementum. Statistically, it increases Anti-OPN expression in alveolar bone, PDL and cementum, and decreases bone mineral density.

## Funding

Self-funded research.

## Ethical statement

The experiment was performed according to guidelines of Ethics Committee, Faculty of Dentistry, Ain Shams University. The ethical approval number is (FDASU-Rec IR042207).

## Declaration of Competing Interest

The authors declare that they have no known competing financial interests or personal relationships that could have appeared to influence the work reported in this paper.

## References

- Abd AlOubaidi, I.A., Hassan, N.A.M., AlShawi, N.N., 2021. Assessment the oxidative stress potential of fluoxetine and amitriptyline at maximum therapeutic doses for four-week treatment in experimental male rats. *Ann. Roman. Soc. Cell Biol.* 25 (6), 17537–17547.
- Agacayak, K.S., Guler, R., Ilyasov, B., 2019. Evaluation of the effect of long-term use of antidepressants in the SSRI group on bone density with dental volumetric tomography. *Drug Des. Develop. Ther.* 13, 3477–3484.
- Aminsobhani, M., Meraji, N., Ghorbanzadeh, A., Ajami, M., Hoseini, S.A.S., Kharazifard, M.J., 2016. Effect of local and application of amitriptyline and imipramine on teeth with irreversible pulpitis failed pulpal anesthesia: a randomized, double-blind, controlled trial. *Dental Hypotheses* 7 (4), 128–132.
- Bancroft, J.D., Suvana, K., Layton, C., 2013. *Bancroft's Theory and Practice of Histological Techniques*. Elsevier, Churchill Livingstone.
- Barbui, C., Hotopf, M., 2001. Amitriptyline v. the rest: still the leading antidepressant after 40 years of randomised controlled trials. *Br. J. Psychiatry* 178, 129–144.
- Boskey, A.L., Spevak, L., Paschalis, E., Doty, S.B., McKee, M.D., 2002. Osteopontin deficiency increases mineral content and mineral crystallinity in mouse bone. *Calcif. Tissue Int.* 71 (2), 145–154.
- Buhagiar, L.M., Casha, M., Grech, A., Micallef, B., Borg, J.J., Inglott, A.S., Laferla, G., 2019. Safety implications of low-dose amitriptyline in neuropathic pain. *Pharmac. Front.* 1 (1), e190003.
- Calarge, C.A., Zimmerman, B., Xie, D., Kuperman, S., Schlechte, J. A., 2010. A cross-sectional evaluation of the effect of risperidone and selective serotonin reuptake inhibitors on bone mineral density in boys. *J. Clin. Psychiatry* 71 (3), 338–347.
- Chaudhry, M., Alessandrini, M., Rademan, J., Dodgen, T.M., Steffens, F.E., Van Zyl, D.G., Gaedigk, A., Pepper, M.S., 2017. Impact of CYP2D6 genotype on amitriptyline efficacy for the treatment of diabetic peripheral neuropathy: a pilot study. *Pharmacogenomics* 18 (5), 433–443.
- Cordero, M.D., Moreno-Fernández, A.M., Gomez-Skarmeta, J.L., de Miguel, M., Garrido-Maraver, J., Oropesa-Avila, M., Rodriguez-



- Hernández, Navas, P., Sánchez-Alcázar, J.A., Coenzyme Q10 and alpha-tocopherol protect against amitriptyline toxicity. *Toxicol. Appl. Pharmacol.* 235, 329–337.
- de Almeida Prado, P.S., Soares, M.F., Lima, F.O., Schor, N., Teixeira, V.P., 2012. Amitriptyline aggravates the fibrosis process in a rat model of infravesical obstruction. *Int. J. Exp. Pathol.* 93 (3), 218–224.
- Denhardt, D.T., Noda, M., O'Regan, A.W., Pavlin, D., Berman, J.S., 2001. Osteopontin as a means to cope with environmental insults: regulation of inflammation, tissue remodeling, and cell survival. *J. ClinInvest.* 107 (9), 1055–1061.
- Diem, S.J., Blackwell, T.L., Stone, K.L., Cauley, J.A., Hillier, T.A., Haney, E.M., Ensrud, K.E., 2011. Use of antidepressant medications and risk of fracture in older women. *Calcif. Tissue Int.* 88 (6), 476–484.
- El Atrash, A., Tousson, E., Gad, A., Allam, S., 2019. Hematological and biochemical changes caused by antidepressants Amitriptyline induced cardiac toxicity in male rats. *Asian J. Cardiol. Res.* 23, 1–6.
- El Saadawy, L.M., Fahmy, R.A., Matrawy, K.A., Zeitoun, M.H., Gaweesh, Y.S., 2019. Relation of cone beam computed tomography assessment of mandibular bone density to dual energy x-ray absorptiometry in type 2 diabetes mellitus patients. *Alexandria Dental J.* 44 (1), 87–92.
- Elsharkawy, G.E.Z., Alhazzazi, T.Y., 2016. The effect of the commonly used antidepressant drug amitriptyline (tcas) on the salivary glands. *J. Dent. Oral Disord. Ther.* 4 (4), 1–5.
- Evans, D.L., Charney, D.S., Lewis, L., Golden, R.N., Gorman, J.M., Krishnan, K.R., et al, 2005. Mood disorders in the medically ill: scientific review and recommendations. *Biol. Psychiatry* 58 (3), 175–189.
- Fisher, L., Fedarko, N., 2003. Six genes expressed in bones and teeth encode the current members of the SIBLING family of proteins. *Connect. Tissue Res.* 44 (Suppl. 1), 33–40.
- Gaballah, O.M., Abd-Elmotelb, M.A., Saleh, R.G., 2018. Distribution of Osteopontin in Normal Dog Periodontium (Immunohistochemical Study). *Life Sci. J.* 15 (7), 25–31.
- Hajhashemia, V., Minaiyana, M., Eftekhari, M., 2008. Anti-inflammatory activity of a selection of antidepressant drugs. *Iran. J. Pharmac. Sci. Summer* 4 (3), 225–230.
- Hanery, E.M., Bliziotis, M.M., 2007. Selective serotonin reuptake inhibitors and bone-health. *Future Rheumatol.* 2 (2), 213–222.
- Haney, E.M., Chan, B.K., Diem, S.J., Ensrud, K.E., Cauley, J.A., Barrett-Connor, E., Orwoll, E., Bliziotis, M.M., et al, 2007. Association of low bone mineral density with selective serotonin reuptake inhibitor use by older men. *Arch. Intern. Med.* 167 (12), 1246–1251.
- Hisaoka, K., Tsuchioka, M., Yano, R., Maeda, N., Kajitani, N., Morioka, N., Nakata, Y., Takebayashi, M., 2011. Tricyclic antidepressant amitriptyline activates fibroblast growth factor receptor signaling in glial cells: involvement in glial cell line-derived neurotrophic factor production. *J. Biol. Chem.* 286 (24), 21118–21128.
- Holm, E., Gleberzon, J.S., Liao, Y., Sørensen, E.S., Beier, F., Hunter, G. K., Goldberg, H.A., 2014. Osteopontin mediates mineralization and not osteogenic cell development in vitro. *Biochem. J.* 464, 355–364.
- Ivanovski, S., Li, H., Haase, H.R., Bartold, P.M., 2001. Expression of bone associated macromolecules by gingival and periodontal ligament fibroblasts. *J. Periodontal Res.* 36 (3), 131–141.
- Kakoei, S., Pardakhty, A., Hashemipour, M.A., Larizadeh, H., Kalantari, B., Tahmasebi, E., 2018. Comparison the pain relief of amitriptyline mouthwash with benzydamine in oral mucositis. *J. Dent. Shiraz Univ. Med. Sci.* 19 (1), 34–40.
- Kim, D.G., 2014. Can dental cone beam computed tomography assess bone mineral density? *J. Bone Metabol.* 212, 117–126.
- Kim, J., Kim, B., Jue, S., Park, J.H., Shin, J., 2012. Localization of osteopontin and osterix in periodontal tissue during orthodontic tooth movement in rats. *Angle Orthod.* 82, 107–114.
- Kinane, D.F., Stathopoulou, P.G., Papapanou, P.N., 2017. Periodontal diseases. *Nat. Rev. Dis. Primers* 3. Article number 17038.
- Madukwe, I.U., 2011. Case report. Anatomy of the periodontium: a biological basis of radiographic evaluation of periradicular pathology. *J. Dent. Oral Hygiene* 6 (7), 70–76.
- Moussavi, S., Chatterji, S., Verdes, E., Tandon, A., Patel, V., Ustun, B., 2007. Depression, chronic diseases, and decrements in health: results from the World Health Surveys. *Lancet* 370, 851–858.
- Mubarak, R., 2012. Cytotoxic and apoptotic effects of chronic amitriptyline administration on rat parotid salivary glands. *J. Am. Sci.* 8 (1), 360–365.
- Ortuño, M.J., Robinson, S.T., Subramanyam, P., Paone, R., Huang, Y.Y., Guo, X.E., Colecraft, H.M., Mann, J.J., Ducy, P., 2016. Serotonin-reuptake inhibitors act centrally to cause bone loss in mice by counteracting a local anti-resorptive effect. *Nat. Med.* 22 (10), 1170–1179.
- Paudel, K.R., Das, B.P., Rauniar, G.P., Sangraula, H., Deo, S., Bhattacharya, S.K., 2007. Antinociceptive effect of amitriptyline in mice of acute pain models. *Indian J. Exp. Biol.* 45, 529–531.
- Rashid, T., Heider, I., 2008. Life events and depression. *Ann. Punjab Med. Coll.* 2 (1), 44–56.
- Rogueira, L.S., Marcelos, P.G., Santiago-Jaegger, I.M., Perez, D.E., Evêncio, J., Neto, B.-E., Baratella-Evêncio, L., 2017. Fluoxetine effects on periodontogenesis: histomorphometrical and immunohistochemical analyses in rats. *J. Appl. Oral Sci.* 25 (2), 159–167.
- Saraykar, S., John, V., Cao, B., Hnatow, M., Ambrose, C.G., Rianon, N., 2018. Association of selective serotonin reuptake inhibitors and bone mineral density in elderly women. *J. Clin. Densit.* 21 (2), 193–199.
- Su, M., Liang, L., Yu, S., 2015. Amitriptyline therapy in chronic pain. *Int. Arch. Clin. Pharmacol.* 1, 1–5.
- Teitelbaum, S.L., 2000. Bone resorption by osteoclasts. *Science* 289, 1504–1508.
- Tousson, E., Zaki, S., Hafez, E., Gad, A., 2018. Biochemical and immunocytochemical studies of the testicular alteration caused by Amitriptyline in adult male rat. *J. Biosci. Appl. Res.* 4 (4), 418–424.
- Venkatesh, E., Elluru, S.V., 2017. Cone beam computed tomography: basics and applications in dentistry. *J. Istanbul Univ. Facul. Dent.* 51 (3 1), 102–121.
- Warden, S.J., Robling, A.G., Haney, E.M., Turner, C.H., Bliziotis, M. M., 2010. The emerging role of serotonin (5-hydroxytryptamine) in the skeleton and its mediation of the skeletal effects of low-density lipoprotein receptor-related protein 5 (LRP5). *Bone* 46, 4–12.
- Yekehtaz, H., Farokhnia, M., Akhondzadeh, S., 2013. Cardiovascular considerations in antidepressant therapy: an evidence-based review. *J. Theran. Heart Center* 8 (4), 169–176.